La radiologia medica (2022) 127:238–250
https://doi.org/10.1007/s11547-022-01452-1

ABDOMINAL RADIOLOGY

MR-enterography: role in the assessment of suspected anastomotic recurrence of Crohn disease after ileocolic resection

Chiara Pozzessere[1,2] · Mourad Boudiaf[3] · Alfredo Cirigliano[1] · Anthony Dohan[3,4] · Maria Antonietta Mazzei[1] · Maxime Barat[3,4] · Luca Volterrani[1] · Philippe Soyer[3,4]

Received: 20 May 2021 / Accepted: 3 January 2022 / Published online: 20 January 2022

Abstract

Purpose To determine the potential of magnetic resonance-enterography (MRE) in the assessment of the anastomotic status in patients with Crohn disease and prior ileocolic resection.

Methods A total of 62 MRE examinations obtained in 52 patients with Crohn disease who had previously undergone ileocolic resection were retrospectively reviewed by two readers in consensus. MRE features (anastomotic wall thickening, wall stratification, wall enhancement pattern and degree, DWI signal intensity, ADC values, lymph nodes, comb sign and complications) were compared to clinical, endoscopic and histological findings that served as standard of reference. Sensitivity, specificity and accuracy of MRE were calculated.

Results At univariate analysis, anastomotic wall thickening, anastomotic wall stratification, segmental wall enhancement, moderate wall enhancement, early and mucosal enhancement, and moderate/marked hyperintensity on diffusion-weighed imaging (DWI) were the most discriminative MRE features for differentiating between normal and abnormal anastomoses ($p < 0.001$ for all variables). Anastomotic wall thickening and segmental anastomotic wall enhancement were the two most sensitive and accurate MRE variables for the diagnosis of abnormal anastomosis with sensitivities of 82% (95% CI: 67–92%) and accuracies of 84% (95% CI: 72–92%). At univariate analysis, hyperintensity on DWI of the anastomotic site was the most sensitive finding for distinguishing between inflammatory recurrence and fibrostenosis (sensitivity, 89%; 95% CI: 67–99%).

Conclusions MRE provides objective and relatively specific morphological criteria that help detect abnormal ileocolic anastomosis, but performances are lower when differentiating between inflammatory recurrence and fibrostenosis. DWI may be useful in identifying pathologic anastomosis and, in particular, in distinguishing between inflammatory recurrence and fibrostenosis.

Keywords Crohn disease · Anastomosis · Surgical · Recurrence · Magnetic resonance imaging · Diffusion

Abbreviations

CI	Confidence interval
CD	Crohn disease
CDAI	Crohn disease activity index
CT	Computed tomography
CTE	CT-enterography
DWI	Diffusion-weighted imaging
GRE	Gradient-recalled echo
MRE	MR-enterography
MRI	Magnetic resonance imaging
OR	Odds ratio
SD	Standard deviation

Luca Volterrani and Philippe Soyer: Joint senior authors.

✉ Chiara Pozzessere
chiara.pozzessere@uslcentro.toscana.it

1 Department of Medical, Surgical and Neuro Sciences, Unit of Diagnostic Imaging, University Hospital of Siena, Azienda Ospedaliera Universitaria Senese, 53100 Siena, Italy

2 Department of Radiology, AUSL Toscana Centro, San Giuseppe Hospital, Viale Giovanni Boccaccio, 16, 50053 Empoli, Italy

3 Department of Radiology, AP-HP Cochin Hospital, 27 rue du Faubourg Saint-Jacques, 5014 Paris, France

4 Université de Paris, 75006 Paris, France

Introduction

Crohn disease (CD) is a chronic bowel inflammatory disease mainly affecting the terminal ileum, characterized by relapses and remissions over time [1]. Although the introduction of immunosuppressive therapies has reduced the risk of relapses and complications, surgery is still required in up to 50% of patients, when medical treatment is ineffective [1–3]. However, the resection of the affected loops is not curative. Endoscopic recurrence at the anastomotic site (*i.e.,* the neo-terminal ileum) may be detected in up to 90% of asymptomatic patients within one year, while symptomatic recurrence affects up to 30% of patient within three years [4]. Moreover, the continuing process of inflammation and healing of the bowel wall may result in fibrotic changes, which may lead to fibrostenosis of the anastomosis. Unlike inflammatory stenosis, fibrostenosis is not sensitive to the anti-inflammatory treatments and requires surgery or endoscopic treatment.

Ileocolonoscopy is the standard of reference in the evaluation of post-surgical recurrence in CD. However, it is restricted to lumen visualization. Imaging modalities such as computed tomography-enterography (CTE), CT-enteroclysis and magnetic resonance-enterography (MRE) are non-invasive and accurate tools for the assessment of CD activity, allowing an overview of both intestinal and extraintestinal manifestations of the disease [5, 6]. MRE is currently the preferred modality owing to the absence of radiation exposure [5, 6]. However, while the role of CT-enteroclysis in post-operative CD has been established, only a few studies have evaluated whether MRE has reliable performances in the evaluation of the anastomotic site and in particular in distinguishing between inflammatory recurrence and fibrostenosis [7–9].

The purpose of this study was to evaluate the accuracy of MRE in the assessment of the anastomotic status in patients with CD who have undergone ileocolic resection.

Materials and methods

Patient population

A retrospective search of the databases of two tertiary referral institutions was performed to retrieve all consecutive patients with CD who underwent MRE from January 2013 to December 2016. This initial search retrieved a total of 279 patients. A search was then performed to identify those who had prior ileocolic resection with ileocolic anastomosis, resulting in 72 patients. Twenty patients were further excluded for the following reasons: (i) MRE and ileocolonoscopy performed more than 10 days of each other ($n=15$); (ii) poor quality of MRE images or lack of small bowel distension (i.e., non-compliant patients, discontinued examination) ($n=4$); and (iii) absence of contrast-enhanced MRE images ($n=1$). Figure 1 shows flowchart of patients into the study.

The study population included 52 patients. For clinical reasons, 6 patients underwent MRE more than once in the study time, with a total of 62 MRE examinations included. On 62 MRE, there were 25 men and 37 women with a mean age of 47 ± 15 (SD) years (range: 25–90 years). Mean time between surgery and MRI was 8 ± 3 (SD) years (range:

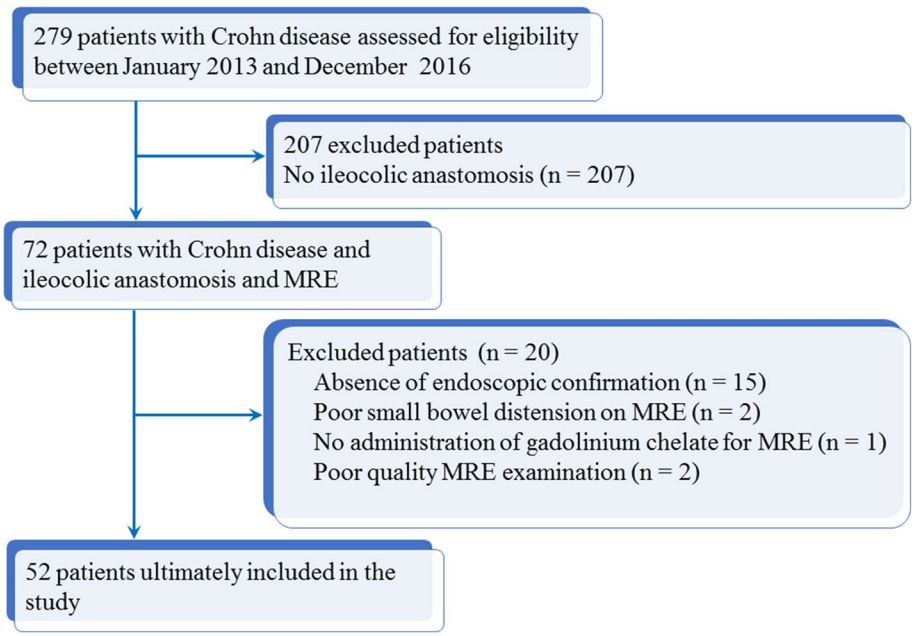

Fig. 1 Study flowchart

5 months–43 years). Mean time between repeated MREs of these six patients was 16 months (range: 11–24 months).

Indications of the 62 MRE examinations were: (i) clinical recurrence in 20/62 (32%); (ii) evaluation of response to therapy in 23/62 (37%); (iii) recurrence as evidenced at endoscopy in 10/62 (16%); (iv) evaluation of fistula and/or abscess in 5/62 (8%); and (v) severe stenosis in 4/62 (6%).

Institutional review board of both institutions approved the study, and a waiver for informed consent was obtained.

MRE protocol

All examinations were performed on 1.5-T magnets (Magnetom®Avanto, BV17Version, Siemens-Healthineers, or Signa®HDx Excite Twin Speed, GE-Healthcare) using a phased-array torso coil. All patients, who were at least 6 h-fasting, were instructed to drink 1000 mL of polyethylene glycol solution (Selg Esse®, Alfasigma or Fortrans®, Ipsen Pharma) in around 40 min at regular intervals to obtain an adequate and homogeneous distension of intestinal loops. To reduce bowel peristalsis, butylscopolamine at a dose of 1 mg i.v. (Buscopan®, Boehrngen) or glucagon at a dose of 1 mg (Glucagen®, Novo-Nordisk) was administrated before MRE examination.

The standard protocol included T2-weighted single-shot, steady state and gradient-echo three-dimensional (3D) T1-weighted sequences in the axial and coronal planes before and after intravenous administration of contrast material (gadoterate meglumine, Dotarem®, Guerbet or Gd-BOPTA Multihance®; Bracco Imaging SpA) at a dose of 0.2 mL/kg body weight and an injection rate of 2 mL/sec at 45 and 75 s after injection. In addition, T2-weighted fat suppressed images were obtained on axial plane. In Institution 1, axial diffusion-weighted images (DWI) were also acquired, representing 37 MRE examinations. MREs were performed with the patient in supine position in Institution 1 and in prone position in Institution 2. No differences in MRE evaluation have been reported using these two different acquisition techniques [10]. Table 1 describes MRE protocols of both institutions.

Imaging analysis

MRE image analysis was performed by two radiologists with 15 (M.B.) and 3 years (C.P.) of experience in MRE working in consensus. Both readers were blinded to clinical history, endoscopic and histologic results. Several MRE findings were evaluated using a standard data collection form, including intestinal and extra-intestinal features [11]. At the end of the reading session, the two radiologists were asked to make a final diagnosis for each MRE examination (*i.e.*, normal anatomosis, inflammatory recurrence or fibrostenosis) using the whole set of sequences for each examination.

Intestinal features included anastomotic wall thickening (> 3 mm) and marked anastomotic wall thickening (> 6 mm) on T2-weighted images, with confirmation on steady state to avoid peristaltic contraction artifacts; wall features on T2-weighted images (wall stratification with hyper-intense intermediate layer or homogenously hypointense wall); presence or absence of wall enhancement on contrast-enhanced T1-weighted images; enhancement pattern (early and mucosal enhancement or progressive and transmural enhancement); degree of bowel wall enhancement, assessed using a 3-point scale as follows: 0) equivalent to that of normal bowel wall; (1) mild enhancement that is greater than that of normal small bowel but markedly

Table 1 MR-enterography protocols for Institution 1 and Institution 2

	Institution 1				Institution 2		
Sequence	True FISP	HASTE T2	GRE 3D T1	DWI b 0, 500, 1000	FIESTA	SSFP T2	GRE 3D T1
Plane	Coronal and axial	Coronal and axial	Coronal and axial	Axial	Coronal and axial	Coronal and axial	Coronal and axial
TR (ms)	3.5	1000	4	4400	6	2000	4
TE (ms)	2	96	2	50	2.5	90	2
Slice thickness (mm)	4	4	4	5	4	4	4
Interslice gap (mm)	1	1	1	5	1	1	1
FOV	40×40	46×46	40×40	35×35	45×45	46×46	40×40
Matrix	256×256	210×320	320×160	192×192	320×256	384×224	320×160
Respiratory Compensation	Free breathing	Free breathing	Breath hold	Breath hold	Free breathing	Free breathing	Breath hold

FISP fast imaging with steady-state precession, *FOV* field of view, *HASTE* half Fourier single shot turbo spin-echo, *GRE* gradient echo, *DWI* diffusion weighted imaging, *FIESTA* fast imaging employing steady-state acquisition, *SSFP* steady-state free precession, *FOV* field of view

less than that of nearby vascular structures; (2) moderate bowel-wall enhancement but somewhat less than that of nearby vascular structures; (3) marked enhancement similar to that of nearby vascular structure [12]; the presence of intestinal complications such as ulcer (a break of the luminal surface of the bowel wall, confined to the bowel wall), pseudo-polyp (projecting lesions of granulation tissue in the luminal surface of the wall bowel due to healing from inflammation), fistula (a simple or complex tract of the bowel wall extending into the mesenteric fat connecting to other loops or structures), or stenosis (a luminal narrowing [*i.e.,* lumen diameter < 12 mm] with dilation of the upstream bowel segment > 30 mm) [11]. When MRE examination included DWI, after identification of the anastomotic site on *b*0 images and confirmation on T2-weighted, *b*1000 images were considered for the assessment of restricted diffusion of anastomotic wall and signal intensity was graded using a 3-point scale as follows: 0) no increased diffusion restriction; (1) mild DWI signal intensity that is similar to but lower than that of lymph nodes; (2) moderate DWI signal intensity, similar from that of lymph nodes; (3) marked DWI signal intensity, higher than that of lymph nodes and the spleen [12]. Finally, apparent diffusion coefficient (ADC) value was calculated on the corresponding ADC map by drawing a region of interest (ROI) at the anastomotic wall. ADC and normalized ADC values (*i.e.*, normalized relative to ADC of cerebrospinal fluid present on the same section) were obtained [12–14].

Extra-intestinal features included presence of reactive lymph nodes (short axis < 10 mm); comb sign (vasa recta hypervascularity, dilatation and tortuosity); perivisceral inflammatory infiltration; abscess (well-defined fluid collection with an enhancing wall) and inflammatory mass (ill-defined solid mesenteric inflammation without fluid component or wall) [11].

The results of the consensus reading were used for further statistical analysis, including diagnostic capabilities of MRE for the identification of normal anastomosis *vs.* abnormal anastomosis and identification of inflammation *vs*. fibrosis.

Standard of reference

The standard of reference for categorizing the status of the anastomotic sites was established by the study coordinator (P.S.) who was not involved in the reading (26 years of experience). The following data were considered as standard of reference: (i) endoscopic features, which were classified using a modified Rutgeerts endoscopic score [15, 16] for 34/62 (55%) examinations; (ii) results of histopathological analysis of biopsy specimens obtained endoscopically at the anastomotic site for 28/62 (45%) examinations; (iii) results of histopathological examination after surgery for 8/62 (13%) examinations. Results of CD activity index (CDAI) and evolution of clinical symptoms, biological variables and endoscopic features after specific treatment were obtained for all examination.

Ileocolonoscopies were performed by board-certified gastroenterologists using standardized procedures, and endoscopic findings were categorized using a modified Rutgeerts score [15]. Histopathological examinations were graded by board-certified pathologists with 20 years of experience in Crohn disease. Inflammation was considered when histopathological analysis or endoscopic examination showed ulcerations in the neo-terminal ileum (Rutgeerts score > 1) [15]. Fibrostenosis was considered when histopathological analysis and endoscopic examination showed anastomotic stricture and no visible ulcerations (Rutgeerts score = 0b) and favorable evolution after endoscopic dilatation of the anastomotic site. Normal anastomosis was considered when histopathological findings or endoscopic features showed no abnormalities (Rutgeerts score = 0a) in combination with CDAI < 150 [16]. For clarity purpose and clinical relevance, anastomotic sites containing a combination of features suggestive of inflammation and fibrosis at histopathological analysis were classified on the basis of the most prominent abnormality (*i.e.*, inflammation *vs.* fibrosis) [9, 15–17].

Statistical analysis

Statistical analysis was performed using "R" statistical software V. 3.2.5 (R Foundation). A primary endpoint was to identify differences among patients diagnosed as either normal, with recurrent disease, or with fibrostenosis.

Descriptive statistics were calculated for all variables evaluated on MRE. Quantitative variables were expressed as means, standard deviations and ranges. Qualitative variables were expressed as raw numbers, proportions and percentages.

To identify MRE variables associated with the diagnosis of normal anastomosis and those associated with abnormal anastomosis, patients with normal anastomosis were compared with those with abnormal anastomosis. To identify MRE variables associated with the diagnosis of recurrence and those associated with the diagnosis of fibrostenotic anastomosis, patients with recurrent disease at the anastomotic site were compared with those with fibrostenotic anastomosis. Categorical (qualitative) variables were compared by the Fisher's exact test. Differences in wall thickness and normalized ADC values were analyzed using Welch *t*-test. The relationships between each MRE variable and the status of the anastomotic site were tested by univariate logistic regression analysis. The odds ratio (OR) and 95% confidence intervals (CIs) for proportions were calculated. All statistical tests were two-tailed, and statistical significance was considered for $p < 0.05$. Sensitivity, specificity, and accuracy were estimated with their 95% CIs for all MRE criteria

for the diagnosis of abnormal anastomosis, recurrence, and fibrostenosis.

Results

Patients

Using the standard of reference, 18/62 (29%) anastomoses were normal without inflammation or stenosis and 44/62 (71%) anastomoses were abnormal, including 36/62 (58%) anastomosis with inflammation and 8/62 (13%) anastomoses with fibrostenosis. Histopathological results were available for 28/62 (45%) MRE examinations and revealed pure inflammation in 13 anastomoses (13/62; 21%), mixed inflammatory and fibrotic changes in 6 anastomoses (6/62; 10%), pure fibrosis in 4 anastomoses (4/62; 6%), whereas no pathologic abnormalities in 5 anastomoses (5/62; 8%). Ileocolonoscopy results were available for 34/62 (55%) MRE examinations and showed pure inflammation in 15 anastomoses (15/62; 24%), fibrotic stenosis in 4 anastomoses (4/62; 6%) and no endoscopic abnormalities in 15 anastomoses (15/62; 24%).

Differentiation between abnormal and disease-free anastomosis

The distribution of MRE findings among the three groups of anastomoses are reported in Table 2. Table 3 shows the association between independent categorical MRE criteria and anastomotic site status, as well as the results of univariate analysis with logistic regression. Mean wall thickening was 5.3 ± 2.4 (SD) mm (range: 2–11 mm). Mean wall thickening of abnormal anastomosis was 6 ± 2.4 (SD) mm (range: 3–11 mm). The most discriminative MRE features for differentiating between normal and abnormal anastomoses were anastomotic wall thickening, anastomotic wall stratification, segmental wall enhancement, moderate wall enhancement, early and mucosal enhancement, and moderate/marked hyperintensity on DWI ($p < 0.001$ for all variables). Anastomotic wall thickening and segmental anastomotic wall enhancement were the two most sensitive and accurate MRE variables for the diagnosis of abnormal anastomosis with sensitivities of 82% (95% CI: 67–92%) and accuracies of 84% (95% CI: 72–92%). The sensitivities, specificities, and accuracies of all MRE variables for correct categorization of the anastomotic site as abnormal or normal are shown in Table 4.

Table 2 Distribution of categorical MR-enterography variables among three groups of patients with Crohn disease and prior ileocolic resection and suspected anastomotic abnormality

Variable	Total $n=62$	Normal $n=18$	Recurrence $n=36$	Fibrosis $n=8$
Anastomotic wall thickening (> 3 mm)	38/62 (61)	2/18 (11)	29/36 (81)	7/8 (88)
Marked anastomotic wall thickening (≥ 6 mm)	25/62 (40)	2/18 (11)	17/36 (47)	6/8 (75)
Anastomotic wall stratification	26/62 (42)	0/18 (0)	21/36 (58)	5/8 (63)
Preanastomotic ileal distension (≥ 30 mm)	7/62 (11)	0/18 (0)	6/36 (17)	1/8 (13)
Anastomotic stenosis (≤ 12 mm)	11/62 (18)	0/18 (0)	9/36 (25)	2/8 (25)
Segmental wall enhancement	38/62 (61)	2/18 (11)	29/36 (81)	7/8 (88)
Mild wall enhancement	15/62 (24)	2/18 (11)	9/36 (25)	4/8 (50)
Moderate wall enhancement	17/62 (27)	0/18 (0)	15/36 (42)	2/8 (25)
Marked wall enhancement	6/62 (10)	0/18 (0)	5/36 (14)	1/8 (13)
Early and mucosal enhancement	30/62 (48)	1/18 (6)	25/36 (69)	4/8 (50)
Progressive and transmural enhancement	8/62 (13)	1/18 (6)	4/36 (11)	3/8 (38)
Hyperintensity on DWI*	23/37 (62)	4/12 (33)	17/19 (89)	2/6 (33)
Mild hyperintensity on DWI*	6/37 (16)	4/12 (33)	2/19 (11)	0/6 (0)
Moderate/marked hyperintensity on DWI*	17/37 (46)	0/12 (0)	15/19 (74)	2/6 (33)
Comb sign	18/62 (29)	2/18 (11)	14/36 (39)	2/8 (25)
Lymph nodes	30/62 (48)	4/18 (22)	21/36 (58)	5/8 (3)
Ulcer	3/62 (5)	0/18 (0)	3/36 (8)	0/8 (0)
Fistula	9/62 (15)	0/18 (0)	7/36 (1)	2/8 (25)
Abscess or inflammatory mass	2/62 (3)	0/18 (0)	1/36 (3)	1/8 (13)
Perivisceral inflammatory infiltration or fluid effusion	4/62 (6)	0/18 (0)	3/36 (8)	1/8 (13)

DWI diffusion-weighted MRI

*DWI was obtained in 37 patients. Numbers in parentheses are percentages. Percentages were averaged without decimal

Table 3 Association between MR-enterography variables and anastomotic site status at univariate logistic regression analysis† in 62 MR-enterography examinations

Variable	Normal anastomosis $n=18$	Abnormal anastomosis $n=44$	OR (95% CI)[§]	p value[†]
Anastomotic wall thickening (> 3 mm)	2/18 (11)	36/44 (82)	0.028 (0.005–0.146)	**< 0.001**
Marked anastomotic wall thickening (≥ 6 mm)	2/18 (11)	23/44 (52)	0.114 (0.023–0.557)	**0.002**
Anastomotic wall stratification	0/18 (0)	26/44 (59)	…	**< 0.001**[‡]
Preanastomotic ileal distension (≥ 30 mm)	0/18 (0)	7/44 (16)	…	0.096[‡]
Anastomotic stenosis (≤ 12 mm)	0/18 (0)	11/44 (25)	…	**0.025**[‡]
Segmental wall enhancement	2/18 (11)	36/44 (82)	0.028 (0.005–0.146)	**< 0.001**
Mild wall enhancement	2/18 (11)	13/44 (30)	0.298 (0.060–1.486)	0.110
Moderate wall enhancement	0/18 (0)	17/44 (39)	…	**0.001**[‡]
Marked wall enhancement	0/18 (0)	6/44 (14)	…	0.168[‡]
Early and mucosal enhancement	1/18 (6)	29/44 (66)	0.030 (0.004–0.251)	**< 0.001**
Progressive and transmural enhancement	1/18 (6)	7/44 (16)	0.311 (0.035–2.270)	0.256
Hyperintensity on DWI*	4/12 (33)	19/25 (76)	0.158 (0.035–0.715)	**0.016**
Mild hyperintensity on DWI*	4/12 (33)	2/25 (8)	5.750 (0.879–37.622)	0.073
Moderate/marked hyperintensity on DWI*	0/12 (0)	17/25 (68)	…	**< 0.001**[‡]
Comb sign	2/18 (11)	16/44 (36)	0.219 (0.044–1.076)	**0.042**
Lymph nodes	4/18 (22)	26/44 (59)	0.198 (0.056–0.700)	**0.008**
Ulcer	0/18 (0)	3/44 (7)	…	0.550[‡]
Fistula	0/18 (0)	9/44 (20)	…	**0.049**[‡]
Abscess or inflammatory mass	0/18 (0)	2/44 (5)	…	> 0.999[‡]
Perivisceral inflammation or fluid effusion	0/18 (0)	4/44 (9)	…	0.313[‡]

Abnormal anastomosis corresponds to inflammatory recurrence or fibrostenosis

DWI diffusion-weighted MRI

*DWI was obtained in 37 patients. Numbers in parentheses are percentages

†Logistic regression analysis. Bold indicates significant *P* value

‡Exact logistic regression analysis values

§Odds ratios (ORs) and corresponding 95% CIs are not shown for some variables because the frequencies of zero values in the corresponding cells led to unstable estimates of those variables

The two observers correctly identified abnormal anastomosis and disease-free anastomosis in 40/44 (90%) and 17/18 (95%) MREs, respectively, while misdiagnosed as pathologic and normal MRE in 1/18 (5%) and 4/44 (10%) MREs, respectively, achieving sensitivity, specificity, and accuracy of 90% (40/44; 95% CI: 80–96%), 95% (17/18; 95% CI: 84–98%), and 92% (57/62; 95% CI: 82–97%), respectively, for the diagnosis of abnormal anastomosis (Fig. 2).

Regarding DWI, among the 37 MREs with DWI, the pathologic anastomoses were correctly identified by restricted diffusion in 19/25 anastomoses (76%). Hyperintensity on DWI was identified in 4/13 (31%) normal anastomoses. Moderate/marked hyperintensity on DWI had 78% accuracy (29/37; 95% CI: 62–90%) and 100% specificity (12/12; 95% CI: 75–100%) for the diagnosis of abnormal anastomosis. Mean ADC value of the anastomotic wall was 1334 ± 213 (SD) mm^2/s (range: 838–$1761 mm^2/s$). Mean ADC value of disease free-anastomosis was 1375 ± 224 (SD) mm^2/s (range: 1118–$1761 mm^2/s$) and that of abnormal anastomosis ADC values was 1620 ± 212 (SD) mm^2/s (range: 1118–$1761 mm^2/s$). Mean normalized ADC value was 0.47 ± 0.12 (SD) (range: 0.27–0.73). Mean normalized ADC value was 0.5 ± 0.1 (SD) (range: 0.42–0.64) for disease free-anastomosis and 0.47 ± 0.1 (SD) (range: 0.27–0.73) for abnormal anastomosis, respectively. No significant differences in ADC values and normalized ADC values were found ($p = 0.34$ and $p = 0.52$, respectively) between normal and pathologic anastomosis.

Inflammatory recurrence vs. fibrosis

The two observers classified the 44 abnormal anastomoses as follows: 32/44 (72%) as inflammatory recurrence, 8/44 (18%) as fibrostenosis, and 4/44 (10%) were misdiagnosed as disease-free anastomoses. Inflammatory recurrence and fibrostenosis were correctly identified on 30/36 (83%) and 6/8 (75%) MREs, respectively, achieving

Table 4 Sensitivity, specificity, and accuracy of MR-enterography categorical variables for the diagnosis of abnormal anastomosis (inflammation or stenofibrosis vs. normal) in 62 MR-enterography examinations

Variable	n	TP†	FP†	FN†	TN†	Se (%)	Sp (%)	Accuracy (%)
Anastomotic wall thickening (> 3 mm)	62	36	2	8	16	82 (36/44) [67–92]	89 (16/18) [65–99]	84 (52/62) [72–92]
Marked anastomotic wall thickening (> 6 mm)	62	23	2	21	16	52 (23/44) [37–68]	89 (16/18) [65–99]	63 (39/62) [50–75]
Anastomotic wall stratification	62	26	0	18	18	59 (26/44) [43–74]	100 (18/18) [81–100]	71 (44/62) [58–82]
Preanastomotic ileal distension (> 30 mm)	62	7	0	37	18	16 (7/44) [7–30]	100 (18/18) [81–100]	40 (25/62) [28–54]
Anastomotic stenosis (< 12 mm)	62	11	0	33	18	25 (11/44) [13–40]	100 (18/18) [81–100]	47 (29/62) [34–60]
Segmental wall enhancement	62	36	2	8	16	82 (36/44) [67–92]	89 (16/18) [65–99]	84 (52/62) [72–92]
Mild wall enhancement	62	13	2	31	16	30 (13/44) [17–45]	89 (16/18) [65–99]	47 (29/62) [34–60]
Moderate wall enhancement	62	17	0	27	18	39 (17/44) [24–55]	100 (18/18) [81–100]	56 (35/62) [43–69]
Marked wall enhancement	62	6	0	38	18	14 (6/44) [5–27]	100 (18/18) [81–100]	39 (24/62) [27–52]
Early and mucosal enhancement	62	29	1	15	17	66 (29/44) [50–80]	94 (17/18) [73–100]	74 (46/62) [62–84]
Progressive and transmural enhancement	62	7	1	37	17	16 (7/44) [7–30]	94 (17/18) [73–100]	39 (24/62) [27–52]
Hyperintensity on DWI*	37	19	4	6	8	76 (19/25) [55–91]	67 (8/12) [35–90]	73 (27/37) [56–86]
Mild hyperintensity on DWI*	37	2	4	23	8	8 (2/25) [1–26]	67 (8/12) [35–90]	27 (10/37) [14–44]
Moderate/marked hyperintensity on DWI*	37	17	0	8	12	68 (17/25) [47–85]	100 (12/12) [74–100]	78 (29/37) [62–90]
Comb sign	62	16	2	28	16	36 (16/44) [22–52]	89 (16/18) [65–99]	52 (32/62) [39–65]
Lymph nodes	62	26	4	18	14	59 (26/44) [43–74]	78 (14/18) [52–94]	65 (40/62) [51–76]
Ulcer	62	3	0	41	18	7 (3/44) [1–19]	100 (18/18) [81–100]	34 (21/62) [22–47]
Fistula	62	9	0	35	18	20 (9/44) [10–35]	100 (18/18) [81–100]	44 (27/62) [31–57]
Abscess or inflammatory mass	62	2	0	42	18	5 (2/44) [1–15]	100 (18/18) [81–100]	32 (20/62) [21–45]
Perivisceral inflammation or fluid effusion	62	4	0	40	18	9 (4/44) [3–22]	100 (18/18) [81–100]	35 (22/62) [24–49]

Se, Sp, and accuracy are expressed as percentages; numbers in parentheses are proportions; numbers in brackets are 95% exact confidence intervals

Se sensitivity, *Sp* specificity

*DWI was obtained in 37 patients

†Data are numbers of MRE examinations with false-negative (FN), false-positive (FP), true-negative (TN), and true-positive (TP) findings

sensitivity, specificity, and accuracy of 83% (30/36; 95% CI: 68%–92%), 75% (6/8; 95% CI: 59%–86%), and 82% (32/44; 95% CI: 66%–91%), respectively, in the diagnosis of anastomotic recurrence against fibrostenosis (Fig. 3). Mean wall thickening of inflammatory recurrence was 5.8 ± 2.4 (SD) mm (range: 3–11 mm), while in fibrostenosis was 7.2 ± 2.5 (SD) mm (range: 3–11 mm). At univariate analysis, hyperintensity of the anastomotic site on DWI was the most sensitive finding for differentiating between recurrence and fibrostenosis (Table 5) and for the diagnosis of recurrent CD at the anastomotic site, achieving sensitivity of 89% (17/19; 95% CI: 67–99%)

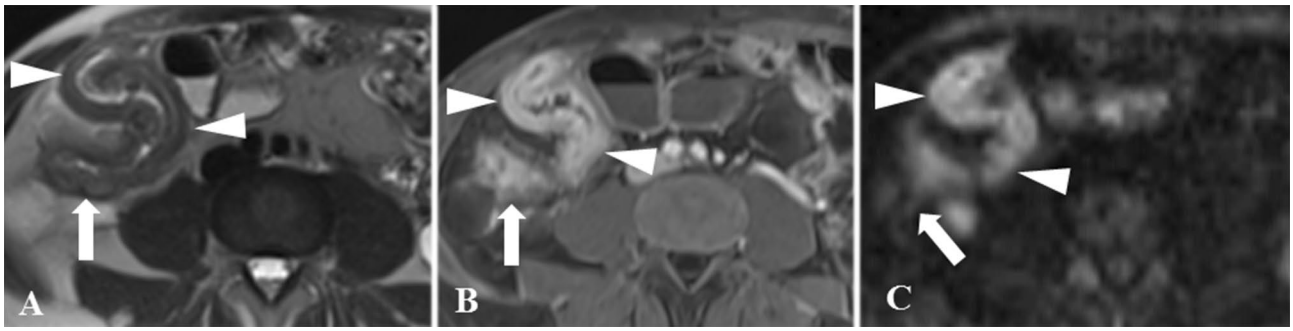

Fig. 2 Histopathologically confirmed inflammatory recurrence of the ileocolic anastomosis in a 45-year-old man with Crohn disease; **a** T2-weighted MR image in the axial plane shows wall thickening and stratification at the anastomotic site (arrow) and of distal ileum (arrowheads), **b** T1-weighted gradient-recalled echo MR image in the axial plane obtained after intravenous administration of a gadolinium chelate shows marked mucosal enhancement at the anastomotic site (arrow) and of distal ileum (arrowheads), **c** Diffusion-weighted MR image in the axial plane reveals marked hyperintensity of the anastomosis wall (arrow) and distal ileum (arrowheads)

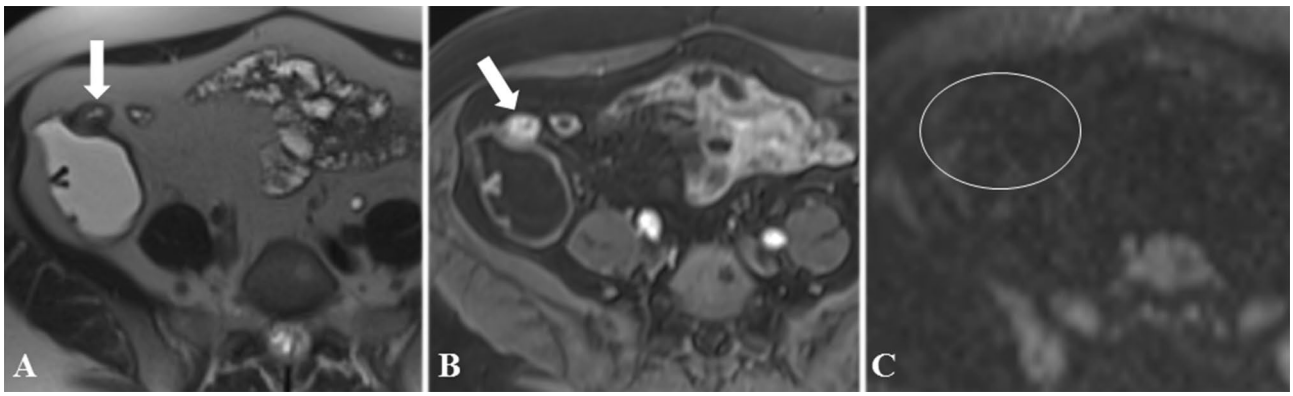

Fig. 3 Histopathologically confirmed fibrostenosis of the ileocolic anastomosis in a 62-year-old woman with Crohn disease. **a** T2-weighted MR image in the axial plane shows homogeneous, hypointense wall thickening (arrow). **b** T1-weighted gradient-recalled echo MR image in the axial plane obtained after intravenous administration of a gadolinium chelate shows "*en bloc*" transmural enhancement (arrow). **c** Diffusion-weighted MR image in the axial plane reveals no hyperintensity at the anastomotic site (circle)

(Table 6). As a note, in one of the two above-mentioned false positive DWI, hyperintensity was secondary to collapsed bowel; moreover, no intra- or extra-intestinal signs of were present such as wall stratification or hyperintensity on T2, either comb sign, while wall enhancement was slight and transmural (Figs. 4, 5).

ADC values were 1331 ± 218 (SD) mm^2/s (range: 838–1636 mm^2/s) for recurrent CD and 1407 ± 191 (SD) mm^2/s (range: 1227–1628 mm^2/s) for fibrostenosis. Mean normalized ADC value was 0.5 ± 0.1 (SD) (range: 0.32–0.73) for inflammatory anastomosis and 0.46 ± 0.1 (SD) (range: 0.27–0.59) for fibrostenosis, respectively. No significant differences between recurrent CD and fibrostenosis were found in ADC and normalized ADC values ($p = 0.96$ and $p = 0.51$, respectively).

Discussion

The present study indicates that MRE as a reliable imaging modality in the assessment of the anastomotic status in patients with CD who previously underwent ileal or ileocolic resection with ileocolic anastomosis. Abnormal ileocolic anastomosis was identified with high accuracy (92%) by two readers in consensus. These rates are similar to those previously reported [18]. Moreover, the most discriminative features for differentiating between normal and abnormal anastomoses such as wall thickening, wall stratification, pattern of wall enhancement and hyperintensity on DWI are included in the most used imaging scores in CD [19, 20]. However, our results differ from those

Table 5 Association between MR-enterography variables and anastomotic site status at univariate logistic regression analysis† (inflammation vs. fibrostenosis) in 44 MR-enterography examinations

Variable	Recurrence	Fibrosis	OR (95% CI)[§]	*p* value[†]
Anastomotic wall thickening (> 3 mm)	29/36 (81%)	7/8 (88%)	0.592 (0.062–5.626)	0.548
Marked anastomotic wall thickening (≥ 6 mm)	17/36 (47%)	6/8 (75%)	0.298 (0.053–1.680)	0.151
Anastomotic wall stratification	21/36 (58%)	5/8 (63%)	0.840 (0.173–4.067)	0.577
Preanastomotic ileal distension (≥ 30 mm)	6/36 (17%)	1/8 (13%)	1.400 (0.144–13.568)	0.624
Anastomotic stenosis (≤ 12 mm)	9/36 (25%)	2/8 (25%)	1.000 (0.170–5.866)	0.687
Segmental wall enhancement	29/36 (81%)	7/8 (88%)	0.592 (0.062–5.626)	0.548
Mild wall enhancement	9/36 (25%)	4/8 (50%)	0.333 (0.069–1.615)	0.164
Moderate wall enhancement	15/36 (42%)	2/8 (25%)	2.143 (0.379–12.112)	0.325
Marked wall enhancement	5/36 (14%)	1/8 (13%)	1.129 (0.113–11.243)	0.703
Early and mucosal enhancement	25/36 (69%)	4/8 (50%)	2.273 (0.479–10.781)	0.257
Progressive and transmural enhancement	4/36 (11%)	3/8 (38%)	0.208 (0.036–1.222)	0.100
Hyperintensity on DWI*	17/19 (89%)	2/6 (33%)	17 (1.809–160.050)	**0.015**
Mild hyperintensity on DWI*	2/19 (11%)	0/6 (0%)		> 0.999[‡]
moderate/marked hyperintensity on DWI*	15/19 (79%)	2/6 (33%)	7.5 (0.991–56.778)	0.059
Comb sign	14/36 (39%)	2/8 (25%)	1.909(0.337–10.822)	0.380
Lymph nodes	21/36 (58%)	5/8 (63%)	0.840 (0.173–4.067)	0.577
Ulcer	3/36 (8%)	0/8 (0%)		> 0.999[‡]
Fistula	7/36 (19%)	2/8 (25%)	0.724 (0.120–4.383)	0.526
Abscess or inflammatory mass	1/36 (3%)	1/8 (13%)	0.200 (0.011–3.592)	0.334
Perivisceral inflammation or fluid effusion	3/36 (8%)	1/8 (13%)	0.636 (0.057–7.054)	0.566

DWI diffusion-weighted MRI

*DWI was obtained in 25 patients

†Logistic regression analysis. Bold indicates significant *P* value

‡Exact logistic regression analysis values

§Odds ratios (ORs) and corresponding 95% CIs are not shown for some variables because the frequencies of zero values in the corresponding cells led to unstable estimates of those variables

reported by Baillet et al. [21]. These researchers have evaluated MREs performed within the first year following surgery, founding a significant correlation between ADC values and the anastomotic status but not for morphological features either enhancement pattern [21]. Conversely, in the present study, the identification of the abnormal anastomosis relied on several findings, such as thickening, stratification and enhancement pattern of the anastomotic wall. A longer time from initial surgery (mean range 8 years) and a consequent longer history of recurrence and remission of CD may account for the discrepancies between the two studies.

In our study, interesting results come from DWI. While hyperintensity on DWI was associated with a specific anastomotic status, moderate/marked restricted diffusion was highly specific in the diagnosis of abnormal anastomosis (100%; $p < 0.001$). Several artifact effects such as inadequately distended loops, peristaltic contractions or spontaneous T2 shine-through of the bowel may contribute to mild signal intensity of normal bowel wall on DWI [22]. Conversely, pathologic anastomosis was likely depicted as moderate/markedly hyperintense on DWI, suggesting that, while the aforementioned artifacts may contribute only to a low signal, real restricted diffusion of the water molecules within the abnormal bowel wall produces more intense signal on DWI. These results may support the utility of DWI in addition to the morphological sequences, and to consider it when gadolinium-based contrast agents cannot be administrated [22–24]. Checking out the corresponding features on T2-weighted and steady state images (*i.e.*, trueFISP and FIESTA) while evaluating the DWI intensity may be helpful in the assessment of the anastomotic status. Differently from the recent study by Strakšytė et al., ADC values were not helpful in this setting, and we partly attribute that to motion artifacts which may occur despite the use of antiperistatical agents [25].

Regarding the performances of MRE in distinguishing between inflammatory recurrence and fibrosis, we found an accuracy of 82% and a specificity of 75%. Nevertheless, these results are in line with those reported in non-previously operated patients with CD [26, 27]. The long history of inflammation and healing affecting the anastomosis over

Table 6 Sensitivity, specificity, and accuracy of MR-enterography categorical variables for the diagnosis of inflammation vs. stenofibrosis in 44 MR-enterography examinations

Variable	n	TP†	FP†	FN†	TN†	Se (%)	Sp (%)	Accuracy (%)
Anastomotic wall thickening (> 3 mm)	44	29	7	7	1	81 (29/36) [64–92]	13 (1/8) [0–53]	68 (30/44) [52–81]
Marked anastomotic wall thickening (> 6 mm)	44	17	6	19	2	47 (17/36) [30–65]	25 (2/8) [3–65]	43 (19/44 [28–59]
Anastomotic wall stratification	44	21	5	15	3	58 (21/36) [41–74]	38 (3/8) [9–76]	55 (24/44 [39–70]
Preanastomotic ileal distension (> 30 mm)	44	6	1	30	7	17 (6/36) [6–33]	88 (7/8) [47–100]	30 (13/44 [17–45]
Anastomotic stenosis (< 12 mm)	44	9	2	27	6	25 (9/36) [12–42]	75 (6/8) [35–97]	34 (15/44 [20–50]
Segmental wall enhancement	44	29	7	7	1	81 (29/36) [64–92]	13 (1/8) [0–53]	68 (30/44) [52–81]
Mild wall enhancement	44	9	4	27	4	25 (9/36) [12–42]	50 (4/8) [16–84]	30 (13/44 [17–45]
Moderate wall enhancement	44	15	2	21	6	42 (15/36) [26–59]	75 (6/8) [35–97]	48 (21/44 [32–63]
Marked wall enhancement	44	5	1	31	7	14 (5/36) [5–30)	88 (7/8) [47–100]	27 (12/44) [15–43]
Early and mucosal enhancement	44	25	4	11	4	69 (25/36) [52–84]	50 (4/8) [16–84]	66 (29/44) [50–80]
Progressive and transmural enhancement	44	4	3	32	5	11 (4/36) [3–26]	63 (5/8) [24–91]	18 (8/44) [8–33]
Hyperintensity on DWI*	25	17	2	2	4	89 (17/19) [67–99]	67 (4/6) [22–96]	84 (21/25) [64–95]
Mild hyperintensity on DWI*	25	2	0	17	6	11 (2/19 [1–33]	100 (6/6) [54–100]	32 (8/25) [15–54]
Moderate/marked hyperintensity on DWI*	25	15	2	4	4	79 (15/19) [54–94]	67 (4/6) [22–96]	76 (19/25) [55–91]
Comb sign	44	14	2	22	6	39 (14/36) [23–57]	75 (6/8) [35–97]	45 (20/44) [30–61]
Lymph nodes	44	21	5	15	3	58 (21/36) [41–74]	38 (3/8) [9–76]	55 (24/44 [39–70]
Ulcer	44	3	0	33	8	8 (3/36) [2–22]	100 (8/8) [63–100]8	25 (11/44) [13–40]
Fistula	44	7	2	29	6	19 (7/36) [8–36]	75 (6/8) [35–97]	30 (13/44 [17–45]
Abscess or inflammatory mass	44	1	1	35	7	3 (1/36) [0–15]	88 (7/8) [47–100]	18 (8/44) [8–33]
Perivisceral inflammation or fluid effusion	44	3	1	33	7	8 (3/36) [2-22]	88 (7/8) [47–100]	23 (10/44) [11–38]

Se, Sp, and accuracy are expressed as percentages; numbers in parentheses are proportions; numbers in brackets are 95% exact confidence intervals

Se sensitivity, *Sp* specificity

*DWI was obtained in 25 patients

†Data are numbers of MRE examinations with false-negative (FN), false-positive (FP), true-negative (TN) and true-positive (TP) findings

time may lead to the simultaneous presence of active inflammation superimposed upon a fibrotic substrate, this affecting the performance of MRE readings, as suggested by Gee et al., using histologic specimens as reference [27]. In our series, superimposed inflammation upon fibrosis was found in 6/28 (21%) histopathological samples, which had led to a combination of inflammatory and fibrotic features on MRE, precluding a correct differentiation in some MRE examinations. Hyperintensity on DWI showed good performances in distinguishing between inflammatory recurrence and fibrostenosis. In particular, visual assessment of DWI accurately identified inflammatory recurrence in 17/19 (89%) of MREs

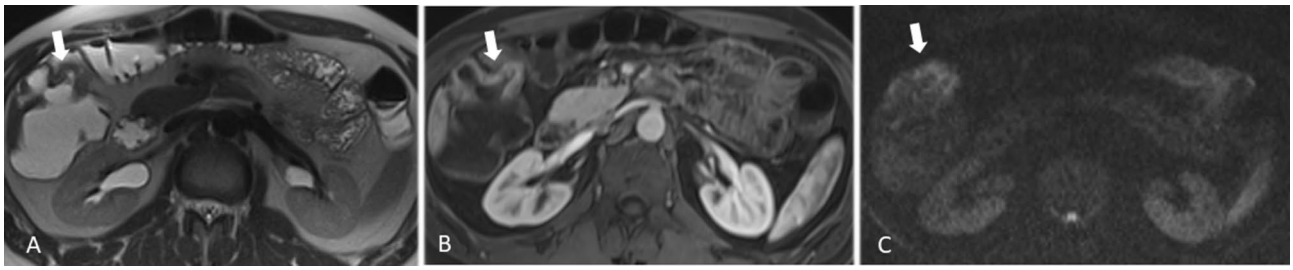

Fig. 4 Histopathologically confirmed inflammatory recurrence of the ileocolic anastomosis in a 35-year-old man with Crohn disease; **a** T2-weighted MR image in the axial plane shows wall thickening and stratification at the anastomotic site (arrow), **b** T1-weighted gradient-recalled echo MR image in the axial plane obtained after intravenous administration of a gadolinium chelate shows moderate transmural enhancement at the anastomotic site (arrow), **c** Diffusion-weighted MR image in the axial plane shows moderate hyperintensity of the anastomosis wall (arrow)

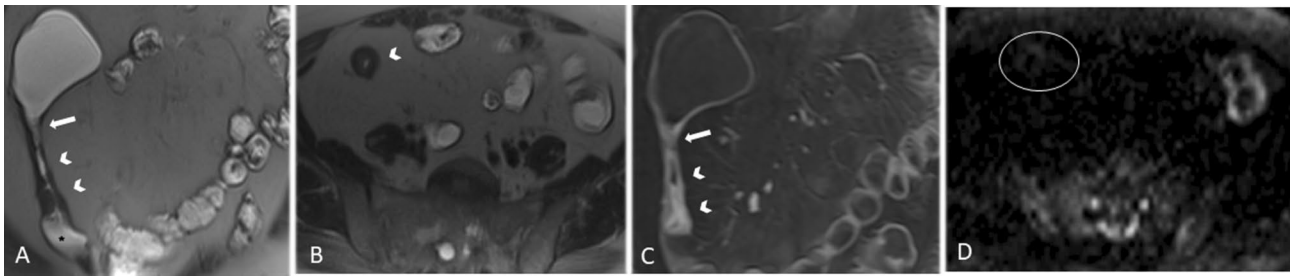

Fig. 5 Histopathologically confirmed fibrostenosis of the ileocolic anastomosis in a 57-year-old woman with Crohn disease. **a** T2-weighted MR image in the coronal plane shows hypointense wall thickening of the anastomotic wall (arrow) and the distal ileum (arrowheads). Dilatation of the upstream bowel segment is also seen (star). **b** T2-weighted MR image in the axial plane at the stenotic level (arrow). **c** T1-weighted gradient-recalled echo MR image in the coronal plane obtained after intravenous administration of a gadolinium chelate shows transmural enhancement at the anastomotic site (arrow) but stratified enhancement at the stenotic level (arrowheads). **d** Diffusion-weighted MR image in the axial plane reveals no hyperintensity at the stenotic level (circle)

for which an actual recurrence was deemed present using the standard of reference. No other variables evaluated in the present study could help differentiate between the two entities, including ADC values.

Our results are different from those reported in studies performed on non-previously operated patients. Prior studies found that many features such as wall stratification, wall thickening, lymph nodes, comb-sign, stenosis of the affected loop and wall enhancement pattern were helpful in distinguish between recurrence and fibrostenosis [20, 26–31]. Several studies reported lower ADC values in fibrotic bowel wall compared to non-fibrotic bowel wall [14, 21, 26, 31, 32]. It may be possible that these differences rely on differences in standard of references, duration of disease and treatments.

A retrospective design, a small sample size, and the lack of histopathological examination in a subset of patients are the major limitations of our study. Histopathological evaluation of the anastomosis should be routinely performed to guide the treatment and to identify malignant lesions arising in stenotic loops [33]. The lack of interobserver variability assessment is another limitation of this study. On the other hand, this is the first study which evaluated the accuracy of MRE in distinguishing between recurrence and fibrostenosis of the ileocolic anastomosis in CD and, in particular, which analyzed DWI among the different imaging parameters. However, the small sample size did not allow a multivariate analysis to evaluate the potential confounding factors. Further studies with a larger sample size and histopathological correlations are required to investigate the possible role of this sequence in the differentiating between anastomosis recurrence and fibrostenosis.

In conclusion, the present study shows that MRE is a reliable imaging modality in assessing ileocolic anastomosis status with high accuracy. Several features are helpful in differentiating between normal and abnormal anastomoses such as wall thickening, wall stratification, wall enhancement pattern, and DWI hyperintensity. However, performances are lower for differentiating between inflammatory recurrence and fibrostenosis, probably due to the concomitance of inflammatory and fibrotic changes in some patients. Pattern of wall enhancement and DWI can be useful in this setting. DWI may be useful in identifying abnormal anastomosis and may have a role in distinguishing between inflammatory

recurrence and fibrostenosis. Further studies are required to deeply investigate the role of DWI in the ileocolic anastomotic status of CD patients.

Funding The authors state that this work has not received any funding.

Availability of data and material Due to the nature of this research, participants of this study did not agree for their data to be shared publicly, so supporting data are not available.

Declarations

Conflict of interest The authors of this manuscript declare no relationships with any companies, whose products or services may be related to the subject matter of the article.

Human and animal rights Additional declarations for articles in life science journals that report the results of studies involving humans and/or animals.

Ethical approval Institutional Review Board approval was obtained.

Consent to participate Written informed consent was waived by the Institutional Review Board.

Consent for publication Obtained by the Institutional Review Board.

References

1. Thia KT, Sandborn WJ, Harmsen WS, Zinsmeister AR, Loftus EV (2010) Risk factors associated with progression to intestinal complications of Crohn's disease in a population-based cohort. Gastroenterology 139(4):1147–1155. https://doi.org/10.1053/j.gastro.2010.06.070
2. Torres J, Bonovas S, Doherty G et al (2020) ECCO guidelines on therapeutics in crohn's disease: medical treatment. J Crohns Colitis 14(1):4–22. https://doi.org/10.1093/ecco-jcc/jjz180 (PMID: 31711158)
3. Sturm A, Maaser C, Calabrese E et al (2019) ECCO-ESGAR guideline for diagnostic assessment in IBD Part 2: IBD scores and general principles and technical aspects. J Crohns Colitis 13(3):273–284. https://doi.org/10.1093/ecco-jcc/jjy114
4. Peyrin-Biroulet L, Loftus EV, Colombel J-F, Sandborn WJ (2010) The natural history of adult Crohn's disease in population-based cohorts. Am J Gastroenterol 105(2):289–297. https://doi.org/10.1038/ajg.2009.579
5. Panes J, Bouhnik Y, Reinisch W et al (2013) Imaging techniques for assessment of inflammatory bowel disease: Joint ECCO and ESGAR evidence-based consensus guidelines. J Crohns Colitis 7(7):556–585. https://doi.org/10.1016/j.crohns.2013.02.020
6. Park SH, Ye BD, Lee TY, Fletcher JG (2018) Computed tomography and magnetic resonance small bowel enterography: current status and future trends focusing on Crohn's disease. Gastroenterol Clin North Am 47(3):475–499. https://doi.org/10.1016/j.gtc.2018.04.002
7. Sailer J, Peloschek P, Reinisch W, Vogelsang H, Turetschek K, Schima W (2008) Anastomotic recurrence of Crohn's disease after ileocolic resection: comparison of MR enteroclysis with endoscopy. Eur Radiol 18(11):2512–2521. https://doi.org/10.1007/s00330-008-1034-6
8. Koilakou S, Sailer J, Peloschek P et al (2010) Endoscopy and MR enteroclysis: equivalent tools in predicting clinical recurrence in patients with Crohn's disease after ileocolic resection. Inflamm Bowel Dis 16(2):198–203. https://doi.org/10.1002/ibd.21003
9. Soyer P, Boudiaf M, Sirol M et al (2010) Suspected anastomotic recurrence of Crohn disease after ileocolic resection: evaluation with CT enteroclysis. Radiology 254(3):755–764. https://doi.org/10.1148/radiol.09091165
10. Masselli G, Gualdi G (2012) MR imaging of the small bowel. Radiology 264(2):333–348. https://doi.org/10.1148/radiol.12111658
11. Guglielmo FF, Anupindi SA, Fletcher JG et al (2020) Small bowel Crohn disease at CT and MR enterography: imaging atlas and glossary of terms. Radiographics 40(2):354–375. https://doi.org/10.1148/rg.2020190091
12. Seo N, Park SH, Kim K-J et al (2016) MR Enterography for the evaluation of small-bowel inflammation in Crohn disease by using diffusion-weighted imaging without intravenous contrast material: a prospective noninferiority study. Radiology 278(3):762–772. https://doi.org/10.1148/radiol.2015150809
13. Soyer P, Kanematsu M, Taouli B et al (2013) ADC normalization: a promising research track for diffusion-weighted MR imaging of the abdomen. Diagn Interv Imaging 94(6):571–573. https://doi.org/10.1016/j.diii.2013.05.003
14. Rosenbaum DG, Rose ML, Solomon AB, Giambrone AE, Kovanlikaya A (2015) Longitudinal diffusion-weighted imaging changes in children with small bowel Crohn's disease: preliminary experience. Abdom Imaging 40(5):1075–1080. https://doi.org/10.1007/s00261-015-0403-2
15. Rutgeerts P, Geboes K, Vantrappen G et al (1990) Predictability of the postoperative course of Crohn's disease. Gastroenterology 99:956–963. https://doi.org/10.1016/0016-5085(90)90613-6
16. Sandborn WJ, Feagan BG, Hanauer SB et al (2002) A review of activity indices and efficacy endpoints for clinical trials of medical therapy in adults with Crohn's disease. Gastroenterology 122:512–530. https://doi.org/10.1053/gast.2002.31072
17. Colombel JF, Solem CA, Sandborn WJ et al (2006) Quantitative measurement and visual assessment of ileal Crohn's disease activity by computed tomography enterography: correlation with endoscopic severity and C reactive protein. Gut 55(11):1561–1567. https://doi.org/10.1136/gut.2005.084301
18. Gallego Ojea JC, Echarri Piudo AI, Porta VA (2011) Crohn's disease: the usefulness of MR enterography in the detection of recurrence after surgery. Radiologia 53(6):552–559. https://doi.org/10.1016/j.rx.2010.10.002
19. D'Amico F, Chateau T, Laurent V, Danese S, Peyrin-Biroulet L (2020) Which MRI score and technique should be used for assessing Crohn's disease activity? J Clin Med 9(6):E1691. https://doi.org/10.3390/jcm9061691
20. Minordi LM, Larosa L, Papa A et al (2020) A review of magnetic resonance enterography classification and quantitative evaluation of active disease in patients with Crohn's disease. Clin Imaging 69:50–62. https://doi.org/10.1016/j.clinimag.2020.06.006
21. Baillet P, Cadiot G, Goutte M et al (2018) Fecal calprotectin and magnetic resonance imaging in detecting Crohn's disease endoscopic postoperative recurrence. World J Gastroenterol 24(5):641–650. https://doi.org/10.3748/wjg.v24.i5.641
22. Dohan A, Taylor S, Hoeffel C et al (2016) Diffusion-weighted MRI in Crohn's disease: current status and recommendations. J Magn Reson Imaging 44(6):1381–1396. https://doi.org/10.1002/jmri.25325
23. Choi SH, Kim KW, Lee JY, Kim K-J, Park SH (2016) Diffusion-weighted magnetic resonance enterography for evaluating bowel inflammation in Crohn's disease: a systematic review and meta-analysis. Inflamm Bowel Dis 22(3):669–679. https://doi.org/10.1097/MIB.0000000000000607

24. Masselli G, De Vincentiis C, Aloi M et al (2019) Detection of Crohn's disease with diffusion images versus contrast-enhanced images in pediatric using MR enterography with histopathological correlation. Radiol med 124:1306–1314. https://doi.org/10.1007/s11547-019-01067-z
25. Strakšytė V, Kiudelis G, Gineikienė I et al (2020) Diffusion-weighted magnetic resonance enterocolonography in assessing Crohn's disease activity. Pol Arch Intern Med 130(9):734–740. https://doi.org/10.20452/pamw.15487
26. Quencer KB, Nimkin K, Mino-Kenudson M, Gee MS (2013) Detecting active inflammation and fibrosis in pediatric Crohn's disease: prospective evaluation of MR-E and CT-E. Abdom Imaging 38(4):705–713. https://doi.org/10.1007/s00261-013-9981-z
27. Gee MS, Nimkin K, Hsu M et al (2011) Prospective evaluation of MR enterography as the primary imaging modality for pediatric Crohn disease assessment. AJR Am J Roentgenol 197(1):224–231. https://doi.org/10.2214/AJR.10.5970
28. Foti PV, Farina R, Coronella M et al (2015) Crohn's disease of the small bowel: evaluation of ileal inflammation by diffusion-weighted MR imaging and correlation with the Harvey-Bradshaw index. Radiol med 120:585–594. https://doi.org/10.1007/s11547-015-0502-8
29. Maccioni F, Staltari I, Pino AR, Tiberti A (2012) Value of T2-weighted magnetic resonance imaging in the assessment of wall inflammation and fibrosis in Crohn's disease. Abdom Imaging 37(6):944–957. https://doi.org/10.1007/s00261-012-9853-y
30. Pupillo VA, Di Cesare E, Frieri G et al (2007) Assessment of inflammatory activity in Crohn's disease by means of dynamic contrast-enhanced MRI. Radiol med 112:798–809. https://doi.org/10.1007/s11547-007-0192-y
31. Tielbeek JAW, Ziech MLW, Li Z et al (2014) Evaluation of conventional, dynamic contrast enhanced and diffusion weighted MRI for quantitative Crohn's disease assessment with histopathology of surgical specimens. Eur Radiol 24(3):619–629. https://doi.org/10.1007/s00330-013-3015-7
32. Kovanlikaya A, Beneck D, Rose M, Renjen P et al (2015) Quantitative apparent diffusion coefficient (ADC) values as an imaging biomarker for fibrosis in pediatric Crohn's disease: preliminary experience. Abdom Imaging 40(5):1068–1074. https://doi.org/10.1007/s00261-014-0247-1
33. Lamb CA, Kennedy NA, Raine T et al (2019) British Society of Gastroenterology consensus guidelines on the management of inflammatory bowel disease in adults. Gut 68:s1–s106. https://doi.org/10.1136/gutjnl-2019-318484